Hydrodynamic Transport Properties of Concentrated Suspensions

Chingyi Chang and Robert L. Powell
Dept. of Chemical Engineering and Materials Science, University of California, Davis, CA 95616

A method of estimating the dependency of the relative viscosities and average sedimentation velocities of particle dispersions on the particle packing behavior, which is related to the shape (sphericity or aspect ratio) of the particle and the ruggedness of the particle surface is proposed. For each ensemble of microstructures, as determined by the flow system in which measurements are made (such as steady shear flow, high-frequency dynamic shear flow, or sedimentation in a static fluid), a single master curve is obtained. These curves allow direct estimates of the relative viscosities or sedimentation velocities to be made if the maximum packing fraction is known.

Introduction

The rheological properties of suspensions of neutrally buoyant solid particles are generally governed by the particle volume fraction, ϕ_v, the particle shape and size distribution, the interparticle forces, the fluid-medium properties, and the flow conditions. For example, in shearing flow a non-Newtonian suspension viscosity results from the effects of viscous forces, surface charge forces, and forces associated with Brownian diffusion (Sengun and Probstein, 1989). At low shear rates, Brownian motion and surface forces are significant and affect the rheological behavior of the suspension. At high shear rates hydrodynamic forces dominate. In this work, we are concerned with the behavior of non-Brownian suspensions. For real systems these are characterized by a large-particle Péclet number $Pe = \mu a^3\dot{\gamma}/kT$, where μ is the suspending fluid viscosity, a is the characteristic particle size, $\dot{\gamma}$ is the shear rate, k is the Boltzmann constant, and T is the absolute temperature (Batchelor and Green, 1972a,b). However, in model systems, it is not necessarily the case that the behavior predicted by models of non-Brownian systems is the same as that predicted at high Péclet numbers (Melrose and Ball, 1995; Catherall et al., 2000). It is also assumed that the particle Reynolds number is much less than one, rendering inertial forces small and relative to viscous forces. In the high shear limit, the suspension viscosity is independent of the shear rate, and if one restricts attention to monodispersed suspensions, the relative viscosity should only be a function of ϕ_v and the particle shape. For bimodal suspensions of spheres, the particle-size ratio, λ, and the fraction of small particles of total solids, ξ, must be considered (Sengun and Probstein, 1992; Chang and Powell, 1993).

Some successful empirical equations have emerged from the realization that a master curve could be obtained for both monodispersed and bimodal suspensions of spherical particles if the data are represented as the relative viscosity as a function of ϕ_v/ϕ_m^{3d}, where ϕ_m^{3d} is the random maximum packing fraction of the suspension in three dimensions. Some examples include (Chong et al., 1971)

$$\eta_r = \left[1 + 0.75\left(\frac{\phi_v/\phi_m^{3d}}{1 - \phi_v/\phi_m^{3d}}\right)\right]^2, \tag{1}$$

and (Tsai et al., 1992; Poslinksi et al., 1988)

$$\eta_r = \left(1 - \frac{\phi_v}{\phi_m^{3d}}\right)^{-2}. \tag{2}$$

In our earlier work (Chang and Powell, 1994a,b), we studied the dependency of the relative viscosity η_r on both ξ and λ for highly concentrated bimodal suspensions of non-Brownian spherical particles. Despite the strong dependency of η_r on both λ and ξ, for a fixed volume fraction of solids, we found that all data fall on a single curve if the relative viscosities were plotted against the normalized volume fraction, ϕ_v/ϕ_m^{3d}. Figure 1 shows the data from our previous experiments, (Chang and Powell, 1994a) and simulations (Chang and Powell, 1993). The results from the simulations are pre-

Correspondence concerning this article should be addressed to R. L. Powell.

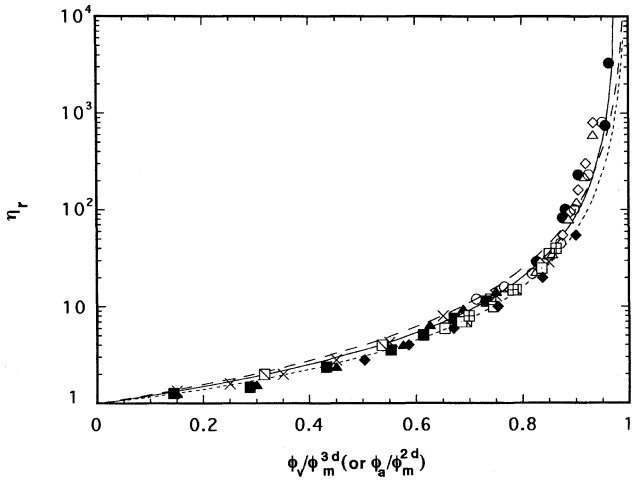

Figure 1. Steady shear relative viscosity as a function of the reduced volume (area) fraction, ϕ_v/ϕ_m^{3d} (ϕ_a/ϕ_m^{2d}).

All volume and area fractions have been normalized by the maximum packing fraction given in Table 1, where the symbols used are also defined. The various lines are predictions of Eqs. 1, 2, and 3. (- - -) Eq. 1; (– –) Eq., 2; (—) Eq. 3.

sented as η_r vs. ϕ_a/ϕ_m^{2d}, where ϕ_m^{2d} is the random maximum packing in two dimensions and ϕ_a is the area fraction. The actual maximum packing values given by the various authors are used in Figure 1 and presented in Table 1. Using the formats suggested by Eqs. 1 and 2, we determined the best curve fit for the data shown in Figure 1 to be

$$\eta_r = \left(1 - 1.033 \pm 0.004 \frac{\phi}{\phi_m}\right)^{-1.80 \pm 0.06} \tag{3}$$

where ϕ may be either ϕ_a or ϕ_v, and ϕ_m is the corresponding maximum packing fraction. The ranges of the constants in Eq. 3 represent the 95% confidence intervals. The small dispersion in the constants, less than 0.4% for the constant multiplying the normalized volume (area) fraction and 3% for the exponent, shows that the fit to the data is quite robust.

Figure 1 provides a comparison of the correlations represented by Eqs. 1–3. Equation 2 tends to overpredict the data throughout the lower concentrations, whereas Eq. 1 describes the data well in this regime. Both Eqs. 1 and 2 underpredict the data at high concentrations. Equation 3 overpredicts slightly at the lower concentrations, but matches the data at high concentrations better than either Eq. 1 or Eq. 2. In this article, we expand upon these observations for suspensions of non-Brownian spherical particles, considering particle shape as well as sedimentation characteristics.

Results

Relative viscosity

The renormalization method used for spherical particle suspensions, that is, plotting the data in terms of (ϕ_v/ϕ_m^{3d}), can be applied to suspensions with differently shaped particles. Figure 2 shows the relative viscosities for suspensions with different types of particles (rods, sand, spheroids, spheres, and so on) in terms of ϕ/ϕ_m, where ϕ/ϕ_m is either ϕ_v/ϕ_m^{3d} or ϕ_a/ϕ_m^{2d}. There are two different master curves in Figure 2. The upper curve gives the viscosity results for suspensions in steady shear flow. It includes the results shown in Figure 1 as well as those obtained for suspensions of sand and rods. The lower curve shows the viscosity results from Monte Carlo simulations of suspensions of prolate spheroids and bimodal populations of spheres (Claeys and Brady, 1993; Chang and Powell, 1994b). These correspond to measurements in high-frequency dynamic viscosity experiments (Phillips et al., 1988), wherein the suspension microstructure is

Table 1. Values of ϕ_m^{3d} and ϕ_m^{2d} for Bimodal Suspensions of Spherical Particles in Figure 1

Reference	λ	ξ	ϕ^{3d}	ϕ_m^{2d}	Symbols
Chong et al. (1971)	2	0.25	0.654		Δ
	3.2	0.25	0.696		◇
	7.2	0.25	0.757		○
Poslinski et al. (1988)	5.2	0.30	0.74		×
	5.2	0.50	0.72		×
Storms et al. (1990)	2.31	0.5	0.635		⧅
	2.96	0.5	0.657		⊡
	4.1	0.5	0.684		⊞
	4.93	0.5	0.696		❑
Shapiro and Probstein (1992)	4	0.5	0.597		◆
Chang and Powell (1993)	2	0.27		0.8	▲
(Dynamic simulation)	4	0.27		0.82	■
Chang and Powell (1994)	2.5	0.25	0.701		●
	7.5	0.25	0.76		●
	13.75	0.25	0.81		●
	2.5	0.5	0.695		●
	7.5	0.5	0.74		●
	13.75	0.5	0.77		●

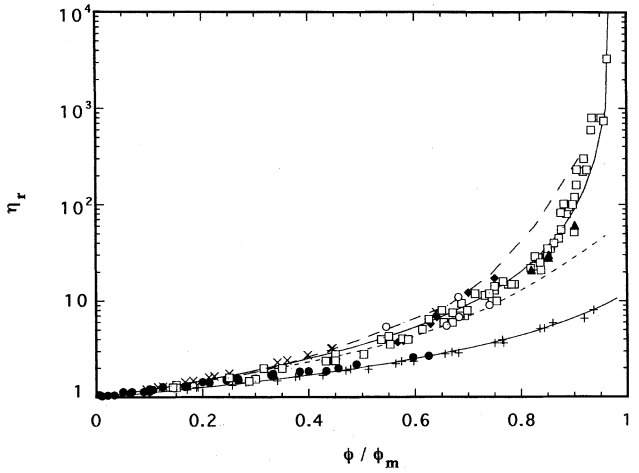

Figure 2. Steady shear and high-frequency dynamic relative viscosities as a function of the reduced volume (area) fraction, ϕ/ϕ_m.

All volume and area fractions have been normalized by the maximum packing fraction given in Table 2, where the symbols used are also defined. Also shown for comparison are the results by Rutgers (1962) (– –) and Thomas (1965) (- - -).

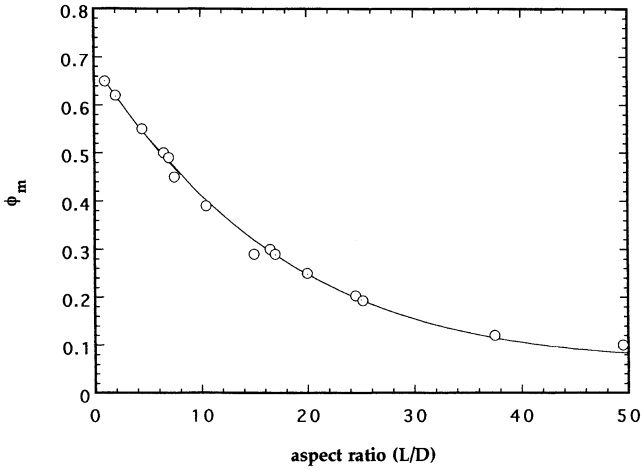

Figure 3. Maximum packing fraction of fibers as a function of the aspect ratio of cylindrical particles (German, 1989).

unaltered by the measurement (Horn et al., 2000). The values of ϕ_m used in obtaining the curves in Figure 2 are given in Tables 1 and 2. Except when ϕ_m was given by the authors (Tsai et al., 1992; Kitano et al., 1981), the maximum packing values were obtained from German (1989), who provides data relating the maximum packing fraction to the aspect ratio (length/diameter) (see Figure 3). In the study of Claeys and Brady (1993), prolate spheroidal particles were used and an equivalent cylindrical shape was assumed in order to obtain ϕ_m from Figure 3. This effective aspect ratio is defined as the elongation of a spheroid with the same period of rotation in simple shear flow as a rod. Using the data for equivalent ellipsoidal and rod-axis ratios given by Goldsmith and Mason (1967) and the empirical formula by Harris and Pittman (1975), namely,

$$r_{eq} = 1.14 r_p^{0.844}, \tag{4}$$

where r_{eq} is the equivalent ellipsoidal axis ratio and r_p is the aspect ratio for a cylinder, and one finds $r_p = 3.15$, 7.15, 13.1, 29.8, and 88.2 for the values of $r_{eq} = 3$, 6, 10, 20, and 50, respectively (Claeys and Brady, 1993).

From the data shown in Figure 2, we have obtained the best curve fit of η_r vs. ϕ/ϕ_m. The curve for steady shear viscosity is represented by Eq. 3, and the curve for the high-

Table 2. Values of ϕ_m^{3d} and ϕ_m^{2d} for Suspensions of Different Type of Particles in Figure 2

Reference	Particle Type	Aspect Ratio	ϕ_m^{3d}	ϕ_m^{2d}	Symbols
Figure 1	Bimodal spheres		Table 1		□
Chang and Powell (1994) (Monte Carlo simul.)	Monomodal spheres			0.785 ($\lambda = 1$)	+
	Bimodal spheres			0.80 ($\lambda = 2$)	+
				0.82 ($\lambda = 4$)	+
Change and Powell (1994) (Dynamic simul.)	Monomodal spheres			0.785 ($\lambda = 1$)	♦
Tsai et al. (1992)	Sand		0.61		▲
Ganani and Powell (1986)	Rods	5	0.54		○
		10	0.41		○
		20	0.27		○
		25	0.22		○
Kitano et al. (1981)	Rods	6&8	0.44		×
		18	0.32		×
		23	0.26		×
		27	0.18		×
Claeys and Brady (1993) (Monte Carlo simul.)	Spheroids	3.15 ($r_{eq} = 3$)	0.58		●
		7.15 ($r_{eq} = 6$)	0.49		●
		13.1 ($r_{eq} = 10$)	0.34		●
		29.8 ($r_{eq} = 20$)	0.17		●
		88.2 ($r_{eq} = 50$)	0.06		●

frequency dynamic viscosity is

$$\eta_r = \left(1.00 - 0.82 \pm 0.04 \frac{\phi}{\phi_m}\right)^{-1.40 \pm 0.12} \tag{5}$$

As compared with constants obtained for the shear flow data, Eq. 3, those in Eq. 5 show much more variation. Still, the variation in the exponent is less than 9%. The results of Rutger (1962) and Thomas (1965) are also shown for comparison. It is interesting to note that the steady shear viscosity data fall between the curves obtained by Rutger (1962) and Thomas (1965).

Two points regarding these correlations should be emphasized. First, independent of the type of particles that make up the suspension (monodispersed or bimodal spheres, rods, sand, or spheroids), the results for steady shear viscosity and high-frequency dynamic viscosity fall on a master curve if plotted as η_r against ϕ/ϕ_m. The difference between these two curves is due to the formation of different suspension microstructures in steady shearing and high-frequency shearing flows (Chang and Powell, 1994b; Horn et al., 2000). Second, the benefit of these curves is that one can estimate the steady shear viscosity and high-frequency dynamic viscosity of a suspension directly if the maximum packing of the suspension is known. For example, if there is a monodispersed suspension of rods with aspect ratio a_r, then from Figure 3 one can obtain the value of ϕ_m with a specific value of a_r. Once the volume fraction is specified, one can calculate ϕ/ϕ_m and use it with Eq. 3 or Eq. 5 to estimate the steady shear and high-frequency dynamic viscosities.

While Eqs. 3 and 5 mainly result from considering idealized suspensions, we note that these relationships open the possibility of estimating the viscosity of a suspension with other particle shapes (such as disks, cubes, rectangles, and so on) from their maximum packing behavior. A convenient way to do this is through the sphericity, which is defined as (German, 1989)

$$\Psi = S_s/S_a \tag{6}$$

where S_s is the surface area of a sphere with the same volume as the test particle, and S_a is the actual surface area of the particle. For example, the sphericity of a cylinder is given as

$$\Psi = 2.621 \frac{\left(\frac{L}{D}\right)^{2/3}}{1 + 2\left(\frac{L}{D}\right)} \tag{7}$$

where L and D are the length and diameter of the cylinder, respectively. Table 3 gives some simple particle shapes and their corresponding sphericities.

Using the value of sphericity, one can estimate the random maximum packing of a monodispersed suspension from the data given by Brown et al. (1950). Warren and German (1988) have obtained a regression equation to link the sphericity to the maximum packing fraction of a powder using the data of Brown et al. (1950)

Table 3. The Sphericity Index for Some Simple Particle Shapes

Shape	Aspect Ratio	Sphericity
Sphere	1	1.00
Cylinder	1	0.87
Cylinder	2	0.83
Disk	5	0.47
Cube		0.81
Rectangle	2×2×1	0.76

$$\psi = 0.079 + 0.831\phi_m + 1.53\phi_m^3 \tag{8}$$

Therefore, the steady shear and high-frequency dynamic viscosities of a monodispersed suspension of nonspherical particles (disks, plates, cubes, rectangles, and so on), is calculated by first determining the sphericity for the specific type of particle. The maximum packing fraction is then found using Eq. 8, and substituted in Eqs. 3 and 5.

In the dilute limit, $\phi \to 0$, both Eqs. 3 and 5 can be made to approach the Einstein relation; however, the maximum packing values required are generally larger than those given in Table 1. In obtaining our correlations, we have sought relationships that are valid over a wide range of concentrations, and, hence, our concern has been to fit the experimental and simulation data globally. At the highest volume fractions, we can compare our correlation with the Frankel and Acrivos (1967) relation

$$\eta_r = \frac{9}{8}\left[\frac{(\phi_v/\phi_m)^{1/3}}{1 - (\phi_v/\phi_m)^{1/3}}\right] \tag{9}$$

which is valid, as $\phi \to \phi_m$. The values provided by Eq. 9 fall between those predicted by Eqs. 3 and 5. This might be due to the assumptions regarding suspension microstructure used to derive Eq. 9. It is also likely that dissipation in pair interactions is too small to be responsible for the observed viscosity values (Gupta, 1994), whereas Stokesian dynamics sums up all of the forces due to many body hydrodynamics as well as considers all lubrication forces between neighboring particles. This results in relatively more viscous dissipation and a higher viscosity.

Sedimentation velocity

Our approach can also be applied to estimate the sedimentation velocity of suspensions of monodispersed nonspherical and spherical particles. Figure 4 shows the relationship between normalized sedimentation velocity of the particles, U/U_0 and ϕ/ϕ_m for monodispersed suspensions of spheres and rods. Here, U is the average settling velocity of the particles, and U_0 the terminal settling velocity of an isolated particle. Again, one can see that the data for U/U_0, also known as the hindered settling function (Davis and Acrivos, 1985), fall onto a single master curve when plotted against ϕ/ϕ_m. The actual maximum packing values used in obtaining the curve in Figure 4 are given in Table 4. Unlike the case of Claeys and Brady (1993), the spheroidal particles used by Mackaplow and Shaqfeh (1998) are not readily related to an equivalent cylindrical shape, since the flow during sedimentation is

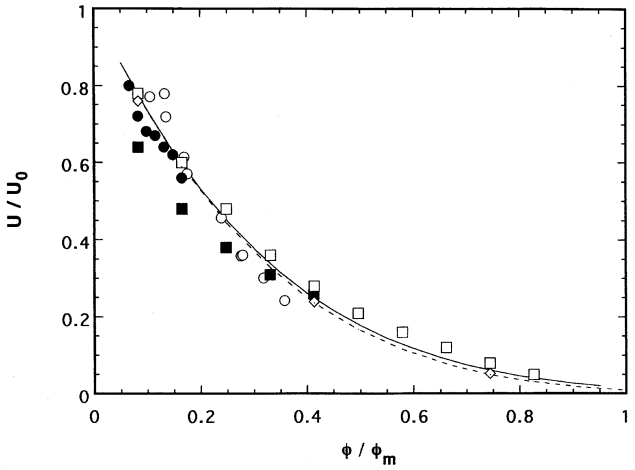

Figure 4. Sedimentation velocity of particles as a function of the reduced volume (area) fraction, ϕ/ϕ_m.

All volume and area fractions have been normalized by the maximum packing fraction given in Table 3, where the symbols used are also defined. Solid line is Eq. 10 with $n = 5.3$; dashed line is Eq. 10 with $n = 5.1$.

not simple shear. Due to the shortage of information on ϕ_m for spheroids, we treat the suspension of spheroids as a suspension of rods (with the same L/D) and use the data in Figure 3 to estimate the maximum packing fraction. We believe this accounts for the slight deviation between the results for spheroids and the master curve in Figure 4. To fit these data, we used a correlation of the form suggested by Richardson and Zaki (1954)

$$\frac{U}{U_0} = \left(1.0 - 0.5\frac{\phi}{\phi_m}\right)^n \tag{10}$$

and obtained $n = 5.3 \pm 0.2$. This is similar to the value of $n = 5.1$ that is found to give the best correlation for spherical particles in the creeping flow regime (Garside and Al-Dibouni, 1977). To estimate the sedimentation velocity of a monodispersed suspension of nonspherical particles (such as disks, cubes, plates, rectangles), one can follow the same procedure as that described earlier for estimating the relative viscosity.

Table 4. Values of ϕ_m^{3d} for Suspensions of Different Type of Particles in Figure 4

Reference	Particle Type	Aspect Ratio	ϕ_m^{3d}	Symbols
Turney et al. (1994)	Rods	17.4	0.31	○
Mackaplow and Shaqfeh (1993)	Spheroids	15.6	0.32	■
Lee et al. (1992)	Spheres		0.605	●
Brady and Durlofsky (1988) (Simul.)	Spheres		0.605	□
Ladd (1993) (Simul.)	Spheres		0.605	◇
Richardson and Zaki (1954)	Spheres		0.605	----

Discussion

Although more experimental data for the relative viscosities and hindered settling functions of nonspherical particles (such as disks, cubes, rectangles) are needed to validate the master curves shown in Figures 2 and 4, these curves serve as a starting point for estimating the hydrodynamic transport properties of concentrated suspensions of nonspherical particles from purely geometrical considerations. In this work, we have assumed that the particles consist of nonrugged (essentially smooth) surfaces (except for the suspension of sand used by Tsai et al., 1992). For real suspensions of nonsmooth particles, additional parameters, such as the fractal dimensions of the particles (Mandelbrot, 1983), can be used to characterize the surface ruggedness. Usually, a particle with a more rugged surface has a higher fractal dimension. Akhter (1982) and Kaye (1989) have shown how fractal dimensions can be used to describe the ruggedness of fine particles (tailings), and they relate these to the magnitude of relative viscosity of the suspension. Suspensions of tailings (sphericities close to that of a sphere) with fractal dimensions $1.3 \sim 1.4$ and suspensions of mono-sized glass beads with fractal dimensions 1.0, had similar relative viscosities up to a volume fraction of approximately 0.15. However, above 0.15 the relative viscosity of the suspensions of tailings increases more rapidly with volume fraction than in the case of suspensions of spherical glass beads. At a volume fraction of 0.22, the viscosity of the suspension of tailings is nearly five times greater than that of the glass-bead suspension. Although Kaye (1989) showed that the relative viscosity of a suspension is directly linked to the surface ruggedness (or fractal dimension) of the particles, he did not obtain a relationship among the relative viscosity, maximum packing fraction, and the fractal dimensions. In the more dilute range, up to $O(\phi_v^2)$, Wilson and Davis (2000, 2002) have examined this question theoretically. They have determined that as a result of the disruption of the lubrication forced between particles, the effect of surface roughness is to decrease the relative viscosity.

Finally, the fractal dimension can only be used to measure the surface ruggedness of a particle, as it fails to describe the shape (aspect ratio or sphericity) of the particle. Therefore, in order to correlate the random maximum packing of a monodispersed suspension to the shape (aspect ratio or sphericity) and surface ruggedness (fractal dimension) of the particles, one would need to measure ϕ_m as a function of aspect ratio (or sphericity) and fractal dimension of the particles.

Acknowledgment

This work was supported by the Chemical Systems Division (CSD) of United Technologies, the Center for Nonlinear Studies of Los Alamos National Laboratory, and by the Department of Energy (DE-FG07-96ER14727). The authors are especially grateful for the encouragement of Dr. R. R. Miller of CSD. One author (R.L.P.) also wishes to thank Thomas Smagala for his help with the statistical analysis of the data.

Notation

a = characteristic particle size
a_r = aspect ratio for a monodispersed suspension of rods

D = the diameter of a cylinder
k = Boltzmann constant
L = the length of a cylinder
P_e = particle Péclet number [$= \mu a^3\dot{\gamma}/kT$]
r_{eq} = equivalent ellipsoidal axis ratio
r_p = aspect ratio of a cylinder [$= L/D$]
S_a = actual surface area of a particle
S_s = surface area of a sphere with the same volume as the test particle
T = absolute temperature
U = average settling velocity of the particles
U_0 = terminal settling velocity of an isolated particle

Greek letters

ϕ_m^{3d} = random maximum packing fraction of the suspension in three dimensions
ϕ_m^{2d} = random maximum packing fraction of the suspension in two dimensions
ϕ_a = area fraction of the suspension
ϕ_m = random maximum packing fraction of the suspension
ϕ_v = volume fraction of the suspension
$\dot{\gamma}$ = shear rate
λ = particle-size ratio
η = viscosity of the suspension
η_r = relative viscosity [$= \eta/\mu$]
μ = viscosity of the suspending fluid
ξ = percentage of small particles of total solids
ψ = sphericity [$= S_s/S_a$]

Literature Cited

Akhter, S. K., "Fine Particle Morphology and the Rheology of Suspensions and Powder Systems," MSc Thesis, Laurentian Univ., Canada (1982).

Batchelor, G. K., and J. T. Green, "The Hydrodynamic Interaction of Two Small Freely-Moving Spheres in a Linear Flow Field," *J. Fluid Mech.*, **56**, 375 (1972a).

Batchelor, G. K., and J. T. Green, "The Determination of the Bulk Stress in a Suspension of Spherical Particles to Order c^2," *J. Fluid Mech.*, **56**, 401 (1972b).

Brady, J. F., and L. J. Durlofsky, "The Sedimentation Rate of Disorder Suspensions," *Phys. Fluid A*, **31**, 717 (1988).

Brown, G. G., A. S. Foust, G. M. Brown, D. L. Katz, L. E. Brownell, R. Schneidewind, J. J. Martin, R. R. White, G. B. Williams, W. P. Wood, J. T. Banchero, and J. L. York, *Unit Operations*, Wiley, New York (1950).

Catherall, A., J. R. Melrose, and R. C. Ball, "Shear Thickening and Order–Disorder Effects in Concentrated Colloids at High Shear Rates," *J. Rheol.*, **44**, 1 (2000).

Chang, C., and R. L. Powell, "Dynamic Simulation of Bimodal Suspension of Hydrodynamically Interacting Spherical Particles," *J. Fluid Mech.*, **253**, 1 (1993).

Chang, C., and R. L. Powell, "Effect of Particle Size Distributions on the Rheology of Concentrated Bimodal Suspensions," *J. Rheol.*, **38**, 85 (1994a).

Chang, C., and R. L. Powell, "The Rheology of Bimodal Hard-Sphere Dispersions," *Phys. Fluid*, **6**, 1628 (1994b).

Chong, J. S., E. B. Christiansen, and A. D. Baer, "Rheology of Concentrated Suspensions," *J. Appl. Polym. Sci.*, **15**, 2007 (1971).

Claeys, I., and J. F. Brady, "Suspension of Proplate Spheroid in Stokes Flow. Part 2. Statistically Homogeneous Dispersions," *J. Fluid Mech.*, **251**, 443 (1993).

Davis, R. H., and A. Acrivos, "Sedimentation of Non-Colloidal Particles at Low Reynolds Numbers," *Annu. Rev. Fluid Mech.*, **17**, 91 (1985).

Frankel, N. A., and A. Acrivos, "On the Viscosity of a Concentrated Suspension of Solid Spheres," *Chem. Eng. Sci.*, **22**, 847 (1967).

Ganani, E., and R. L. Powell, "Rheological Behavior of Rodlike Particles in Newtonian and Non-Newtonian Fluids," *J. Rheol.*, **30**, 995 (1986).

Garside, J., and M. R. Al-Dibouni, "Velocity-Voidage Relationship for Fluidization and Sedimentation in Solid-Liquid Systems," *Ind. Eng. Chem. Process Des. Dev.*, **16**, 206 (1977).

German, R. M., *Particle Packing Characteristics*, Metal Powder Industries Federation, Princeton, NJ (1989).

Goldsmith, H. L., and S. G. Mason, *Rheology*, Vol. 4, F. Eirich, ed., Academic Press, New York (1967).

Gupta, R. K., "Particulate Suspensions," *Flow and Rheology in Polymer Composites Manufacturing*, S. G. Advani, ed., Plenum, New York (1994).

Harris, J. B., and J. F. T. Pittman, "Equivalent Ellipsoidal Axis Ratios of Slender Rod-Like Particles," *J. Colloid Interface Sci.*, **50**, 280 (1975).

Horn, F. M., W. Richtering, J. Bergenholtz, N. Willenbacher, and N. J. Wagner, "Hydrodynamic and Colloidal Interactions in Concentrated Charge-Stabilized Polymer Dispersions," *J. Colloid Interface Sci.*, **225**, 166 (2000).

Kaye, B. H., *Random Walk Through Fractal Dimensions*, VCH, New York (1989).

Kitano, T., T. Kataoka, and T. Shirota, "An Empirical Equation of the Relative Viscosity of Polymer Melts Filled with Various Inorganic Fillers," *Rheol. Acta*, **20**, 207 (1981).

Ladd, A. J. C., "Dynamic Simulations of Sedimenting Spheres," *Phys. Fluid A*, **5**, 299 (1993).

Lee, S., Y. Jang, C. Choi, and T. Lee, "Combined Effect of Sedimentation Velocity Fluctuation and Self-Sharpening on Interface Broadening," *Phys. Fluid A*, **4**, 2601 (1992).

Mackaplow, M., and E. S. G. Shaqfeh, "A Numerical Study of the Sedimentation of Fibre Suspensions," *J. Fluid Mech.*, **376**, 149 (1998).

Mandelbrot, B. B., *The Fractal Geometry of Nature*, Freeman, San Francisco (1983).

Melrose, J. R., and R. C. Ball, "The Pathological Behavior of Sheared Hard-Spheres With Hydrodynamic Interactions," *Europhys. Letts.*, **32**, 535 (1995).

Phillips, R. J., J. F. Brady, and G. Bossis, "Hydrodynamic Transport Properties of Hard-Sphere Dispersions. I. Suspensions of Freely Mobile Particles," *Phys. Fluids*, **31**, 3462 (1988).

Poslinski, A. J., M. E. Ryan, P. K. Gupta, S. G. Seshadri, and F. J. Frechette, "Rheological Behavior of Filled Polymeric Systems. 2. The Effect of a Bimodal Size Distribution of Particulates," *J. Rheol.*, **32**, 751 (1988).

Richardson, J. F., and W. N. Zaki, "Sedimentation and Fluidization: I," *Trans. Inst. Chem. Eng.*, **32**, 35 (1954).

Rutger, R., "Relative Viscosity of Suspensions of Rigid Spheres in Newtonian Liquids," *Rheol. Acta*, **2**, 202 (1962).

Sengun, M. Z., and R. F. Probstein, "Bimodal Model of Slurry Viscosity with Application to Coal-Slurries. Part 1. Theory and Experiment," *Rheol. Acta*, **28**, 382 (1989).

Shapiro, A. P., and R. F. Probstein, "Random Packing of Spheres and Fluidity Limits of Monodisperse and Bidispherse Suspensions," *Phys. Rev. Lett.*, **68**, 1422 (1992).

Storms, R. F., B. V. Ramarao, and R. H. Weiland, "Low Shear Rate Viscosity of Bimodally Dispersed Suspensions," *Powder Technol.*, **63**, 247 (1990).

Thomas, D. G., "Transport Characteristics of Suspension: VIII. A Note on the Viscosity of Newtonian Suspension of Uniform Spherical Particles," *J. Colloid Sci.*, **20**, 267 (1965).

Tsai, S. C., D. Botts, and J. Plouff, "Effects of Particle Properties on the Rheology of Concentrated Noncolloidal Suspensions," *J. Rheol.*, **36**, 1291 (1992).

Turney, M. A., M. K. Cheung, R. L. Powell, and M. J. McCarthy, "Hindered Settling of Rod-Like Particles Measured with Magnetic Resonance Imaging," *AIChE J.*, **41**, 251 (1995).

Warren, J., and R. M. German, *Modern Developments in Powder Metallurgy*, Vol. 18, P. U. Gummerson and D. A. Gustafson, eds., Metal Powder Industries Federation, Princeton, NJ (1988).

Wilson, H. J., and R. H. Davis, "The Viscosity of a Dilute Suspension of Rough Spheres," *J. Fluid Mech.,* **421**, 339 (2000).

Wilson, H. J., and R. H. Davis, "Shear Stress of a Monolayer of Rough Spheres," *J. Fluid. Mech.*, **452**, 425 (2002).

Manuscript received Sept. 29, 2000, and revision received Apr. 10, 2002.